International Journal of Engineering Research-Online
A Peer Reviewed International Journal
ISSN: 2321-7758 http://www.ijoer.in editorijoer@gmail.com
Vol.14., S1, 2026
January

Special issue

ISSN: 2321-7758

Molecular Dynamics Simulations of Carbon-Based Materials: Mechanical Strength, Thermal Conductivity, and Atomic-Level Interactions for Energy Storage Applications

Dr. Kandula Anjaneyulu[1], Kanta Jayadev[2]

[1] Principal (FAC), Pithapur Rajahs Government College (Autonomous), Kakinada, Andhra Pradesh, India

[2] Lecturer in Physics, Pithapur Rajahs Government College (Autonomous), Kakinada, Andhra Pradesh, India

DOI: 10.33329/ijoer.14.S1.193

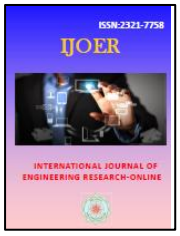

Abstract

Molecular dynamics (MD) simulations have become an essential computational framework for examining the structure-property relationships of carbon-based nanomaterials in energy storage applications. This thorough review brings together the most recent (2020–2024) improvements in MD methods for predicting the mechanical strength, thermal conductivity, and atomic-level interactions of graphene, carbon nanotubes, and their derivatives. Pristine graphene has amazing mechanical properties, with a Young's modulus of 1.0 TPa and a tensile strength of 130 GPa. The thermal conductivity values range from 2900 to 5000 W/m·K, depending on the quality of the sample and the conditions at the boundary. One important thing that this review found is that choosing the right interatomic potential can change predictions of thermal conductivity by as much as four times. Optimised Tersoff potentials are better for phonon transport, while AIREBO is still the best choice for fracture mechanics. Machine learning potentials, especially GAP-20, now reach over 95% of density functional theory accuracy at a much lower cost of computation. MD simulations show that carbon nanotubes with titanium on them can store hydrogen at a rate of 8.04 wt% at 77 K. The lithium diffusion coefficients in graphite range from 10^{-6} to 10^{-11} cm^2/s, depending on the pathway of diffusion. Defect concentrations as low as 0.1% can cut thermal conductivity by 83%. This shows how important it is to engineer defects. This review highlights significant research deficiencies, including multiscale bridging methodologies, reactive potentials for solid-electrolyte interfaces, and standardised validation protocols crucial for the progression of computational design in next-generation energy storage materials.

Keywords: Molecular dynamics, Carbon nanomaterials, Graphene, Carbon nanotubes, Thermal conductivity, Mechanical properties, Energy storage, Interatomic potentials, AIREBO, Machine learning potentials.

1. Introduction

The world needs big changes in energy storage technologies that can support intermittent renewable sources, electric transportation, and grid-scale applications [1-3]. Carbon-based nanomaterials have become essential for the next generation of energy storage devices because they have a unique combination of properties that make them good at conducting electricity, being strong, and being stable in chemicals [4–6]. Graphene has the highest known thermal conductivity (about 5000 W/m·K), the best electron mobility (200,000 $cm^2/V \cdot s$), and the best mechanical strength (Young's modulus of 1 TPa) [7-9]. Carbon nanotubes (CNTs), including both single-walled and multi-walled types, enhance these characteristics with their high aspect ratios, which allow for effective reinforcement and unique one-dimensional transport phenomena [10–12].

Molecular dynamics simulation has emerged as the foremost computational technique for examining atomic-scale phenomena that influence macroscopic material behaviour [13-15]. MD explicitly resolves individual atomic trajectories through numerical integration of Newton's equations of motion, capturing intrinsic length scales, thermal fluctuations, and defect interactions inaccessible to experimental characterisation, unlike continuum approaches that treat materials as homogeneous media [16,17]. The exponential growth of computational resources, along with improvements in parallelisation and machine learning algorithms, has made MD able to handle billions of atoms instead of just thousands. This has closed the gap between basic quantum mechanical descriptions and predictions on an engineering scale [18–20].

Using MD simulations on carbon nanomaterials for energy storage answers a number of important scientific questions. First, how do atomic-level defects, which are common in synthesised materials, affect mechanical integrity and thermal transport in a measurable way? Second, what are the basic processes that control ion diffusion, intercalation, and charge storage in carbon electrodes? Third, how can computer-based predictions help us design carbon-based composites with the best possible multifunctional properties? This review methodically addresses these enquiries through an extensive analysis of contemporary literature concerning mechanical properties, thermal conductivity, interatomic potential development, and particular energy storage applications [21-24].

This review examines MD simulation studies published from 2020 to 2024, concentrating on carbon allotropes such as graphene (both monolayer and multilayer), carbon nanotubes (single-walled and multi-walled), graphite, and functionalised derivatives. Lithium-ion battery anodes, supercapacitor electrodes, hydrogen storage media, and thermal management materials are all examples of energy storage applications that are specifically mentioned. The review is structured as follows: Section 2 delineates computational methodologies encompassing simulation frameworks and analytical techniques; Section 3 scrutinises predictions of mechanical properties; Section 4 tackles calculations of thermal conductivity; Section 5 rigorously assesses interatomic

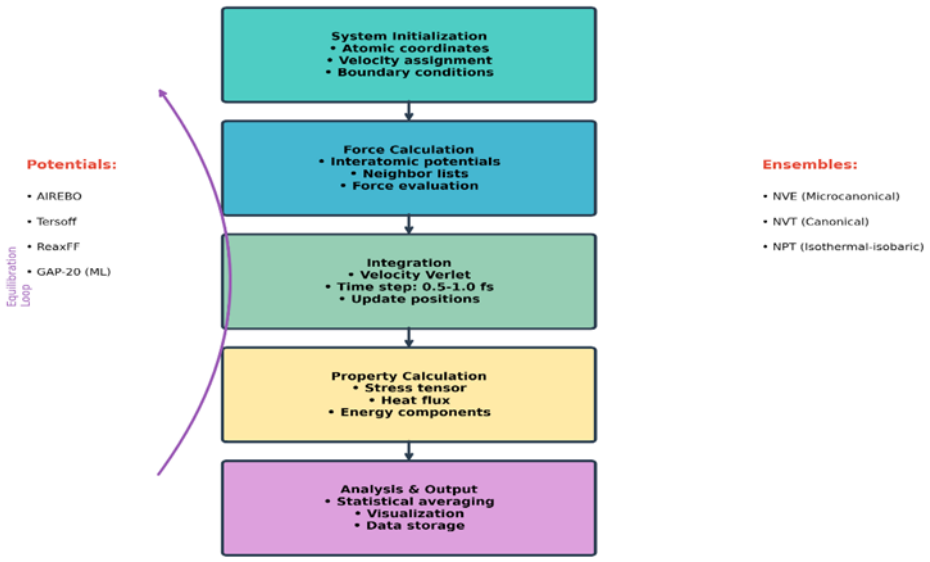

Figure 1: Molecular Dynamics simulation framework for carbon-based materials showing the iterative computational workflow including system initialization, force calculation, integration, property evaluation, and analysis stages.

potentials; Section 6 explores energy storage applications; Section 7 delineates prospective research trajectories; and Section 8 offers concluding observations [25-27].

2. Computational Methodology

2.1 Molecular Dynamics Simulation Framework

The basic idea behind molecular dynamics simulation is to solve Newton's equations of motion for a group of N particles that are interacting with each other. The force on each atom comes from the gradient of an interatomic potential energy function [28,29]. The temporal evolution of atomic positions and velocities is achieved through numerical integration algorithms, with the velocity Verlet scheme being the most commonly used method due to its symplectic characteristics that maintain phase space volume and demonstrate exceptional energy conservation [30]. For empirical potentials, carbon simulations usually have time steps between 0.5 and 1.0 femtoseconds. This makes sure that high-frequency C-C bond vibrations with periods of about 30 fs are accurately resolved [31,32].

The Large-scale Atomic/Molecular Massively Parallel Simulator (LAMMPS) is the most popular tool for carbon MD simulations. It uses the MANYBODY package (Tersoff, AIREBO, REBO, LCBOP) and the REAXFF module for reactive chemistry to provide the best implementations of important interatomic potentials [33,34]. Using the KOKKOS package to speed up GPU execution can make it 2 to 8 times faster than CPU-only execution. The NVIDIA H100 architecture shows big improvements, especially for Tersoff and ReaxFF calculations [35]. Alternative codes, such as GROMACS, are used in carbon-polymer composite systems where classical force fields can accurately describe interactions that aren't bonded [36,37].

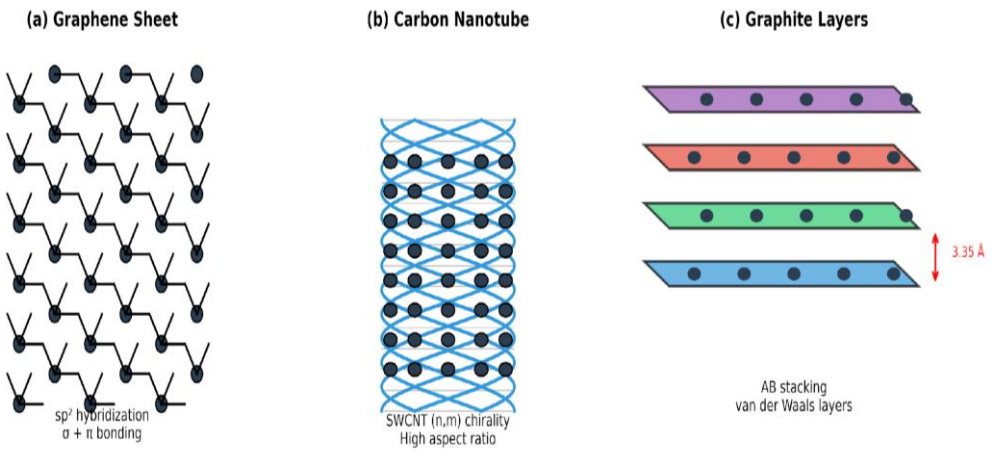

Figure 2: Carbon nanostructures for energy storage applications: (a) Graphene sheet with sp² hybridized carbon atoms in honeycomb lattice, (b) Single-walled carbon nanotube with helical atomic arrangement, (c) Graphite layers with AB stacking and 3.35 Å interlayer spacing.

2.2 *Statistical Ensembles and Thermostats*

Statistical mechanical ensembles delineate the macroscopic constraints governing the evolution of simulations. The microcanonical (NVE) ensemble keeps the total energy the same, which lets us check the accuracy of integration by watching for energy drift. Drift rates that are less than 0.01% over production runs are acceptable [38]. The canonical (NVT) ensemble keeps the temperature steady by connecting thermostats. The Nosé-Hoover chain method is the best way to do this for production simulations because it makes sure that the canonical sampling is correct and doesn't cause the flying ice cube artefact that happens when you change the speed [39,40]. The isothermal-isobaric (NPT) ensemble also controls pressure, which is important for studying phase transitions and finding equilibrium lattice parameters. However, two-dimensional materials like graphene need to have their out-of-plane dimension limited to stop them from collapsing in an unphysical way [41,42].

Table 1: Recommended MD Simulation Parameters for Carbon Nanomaterials

Parameter	Mechanical	Thermal	Diffusion	Reference
Time step (fs)	1.0	0.5	1.0	[31,32]
Minimum atoms	2,000-5,000	5,000-50,000	1,000-10,000	[43,44]
Production time (ns)	1-10	10-50	1-100	[45,46]
Ensemble	NVT/NPT	NVE/NVT	NVT	[38-42]
Thermostat	Nosé-Hoover	Nosé-Hoover	Nosé-Hoover	[39,40]

3. Mechanical Properties from MD Simulations

3.1 Elastic Constants and Tensile Strength

Molecular dynamics simulations consistently indicate remarkable mechanical properties for pristine carbon nanomaterials, positioning them among the strongest known substances. Graphene's Young's modulus values range from 0.83 to 1.05 TPa, depending on the conditions of the simulation and the choice of potential. This is very close to the experimental benchmark of 1.0 ± 0.1 TPa set by Lee et al. through atomic force microscopy nanoindentation [47-49]. Predictions for tensile strength range from 93 to 137 GPa, with a lot of directional anisotropy. For example, loading in a zigzag pattern gives higher strength (106-137 GPa) and fracture strain (0.20-0.27) than loading in an armchair pattern (93-105 GPa, strain 0.14-0.17). This is because of the symmetry of the lattice and the orientation of the bonds [50-52].

Through a combination of experiments and computer simulations, it has been shown that graphene has a fracture toughness of 4.4 MPa·√m. The ratio Gc(armchair)/Gc(zigzag) = 0.94 shows that the material is weakly anisotropic [53,54]. Single-walled carbon nanotubes have Young's moduli of 1.0–1.2 TPa and theoretical tensile strengths of 94–126 GPa, depending on their chirality and diameter [55,56]. However, the measured strengths of synthesised samples with defects drop a lot, from 13 to 53 GPa for individual SWCNTs to 34.65 GPa for millimeter-long MWCNT bundles [57,58].

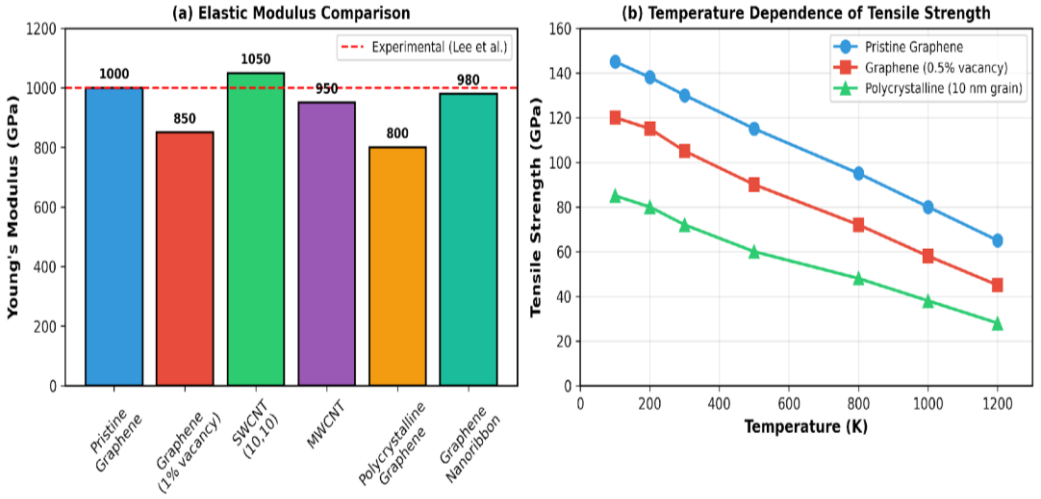

Figure 3: Mechanical properties of carbon nanomaterials from MD simulations: (a) Young's modulus comparison across different carbon structures, (b) Temperature dependence of tensile strength showing thermal softening behavior.

3.2 Temperature and Strain Rate Effects

Temperature significantly impacts mechanical behaviour via thermally activated processes that influence bond stability and defect mobility. The strength of polycrystalline graphene diminishes by about 45% from 100 K to 1200 K, with a transition from brittleness to plasticity occurring above 1000 K, where increased atomic mobility facilitates dislocation-mediated deformation [59,60]. The temperature coefficient of Young's modulus shows a weak dependence, dropping by 5–10% for every 500 K rise in temperature. This is because sp^2 carbon has stiff covalent bonds [61,62].

Strain rate sensitivity poses methodological difficulties, as molecular dynamics simulations utilise rates (10^7-10^{10} s^{-1}) that are orders of magnitude greater than those in experimental conditions (10^{-3}-10^0 s^{-1}). Systematic studies show that zigzag orientations are more sensitive to strain rates than armchair configurations. For example, in polycrystalline

graphene at 300 K, the strength increases by 10% when the strain rate goes from 5×10^{-5} to 5×10^{-3} ps^{-1} [63,64]. Transition state theory and accelerated MD methods are two ways to try to fill this gap in time scales, but it is still hard to prove that they work [65,66].

Table 2: Mechanical Properties of Carbon Nanomaterials from MD Simulations

Material	E (GPa)	σ (GPa)	ε_f	Potential	Ref.
Graphene (armchair)	890-961	93-105	0.14-0.17	AIREBO	[47-50]
Graphene (zigzag)	830-911	106-137	0.20-0.27	AIREBO	[47-50]
SWCNT (10,10)	1000-1200	94-126	0.15-0.20	Tersoff	[55-58]
Polycrystalline (10 nm)	~800	~50	~0.08	AIREBO	[59,60]
Graphene (1% vacancy)	~850	~90	~0.12	AIREBO	[67,68]

4. Thermal Conductivity Calculations

4.1 Computational Methods

There are two very different ways to predict thermal conductivity using molecular dynamics, each with its own strengths and weaknesses [69,70]. The equilibrium molecular dynamics (EMD) method, which is based on the Green-Kubo formalism, calculates thermal conductivity by taking the time integral of heat flux autocorrelation functions in equilibrium. This method has less of an effect on finite size than non-equilibrium methods, and it naturally captures the full tensor character of anisotropic conductivity, which makes it better for determining bulk properties [71,72]. However, convergence problems come up because heat flux in materials with high conductivity, like graphene, takes a long time to decorrelate. This means that simulations have to run for more than 100 ps and be carefully analysed statistically [73,74].

Non-equilibrium molecular dynamics (NEMD) techniques apply temperature gradients through thermostatted boundary regions, quantifying steady-state heat flux to ascertain conductivity in accordance with Fourier's law [75,76]. The reverse NEMD method by Müller-Plathe is more stable because it moves kinetic energy between hot and cold areas, which causes temperature gradients instead of forcing them [77]. NEMD methods are great for looking at interfacial thermal resistance (Kapitza resistance) because they let you see how temperature profiles change in space, which gives you direct access to interface contributions. However, system size effects need to be carefully corrected by extrapolating to infinite length [78,79].

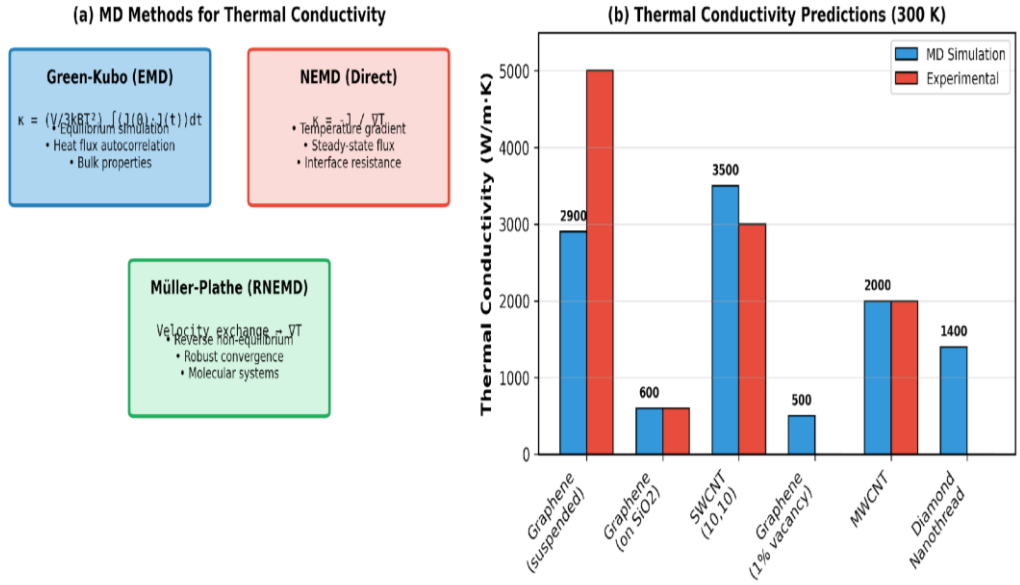

Figure 4: Thermal conductivity analysis: (a) Comparison of MD computational methods including Green-Kubo equilibrium MD and non-equilibrium approaches, (b) Thermal conductivity predictions at 300 K compared with experimental measurements.

4.2 Thermal Conductivity Results

Graphene has the highest thermal conductivity of any known material. Balandin and his coworkers measured suspended samples at room temperature and found values between 4840 and 5300 W/m·K [80]. MD simulations utilising optimised Tersoff potentials forecast values of 2903 ± 93 W/m·K through EMD methods, indicating a reasonable concordance considering the sensitivity to simulation parameters and finite-size effects. Substrate-supported graphene exhibits significantly diminished conductivity, approximately 600 W/m·K, attributed to phonon scattering at the interface, a prediction robustly corroborated by experimental data.

The transition between ballistic and diffusive transport regimes, which is important for managing the heat of nanostructures, is controlled by phonon mean free paths. Suspended graphene has mean free paths of about 240 nm at room temperature, which allows for quasi-ballistic transport in samples that are shorter than this length. Quarter-micron samples attain roughly 35% of the ballistic thermal conductance limit, illustrating the practical significance of finite-size effects. Carbon nanotubes show similar thermal conductivity, with defect-free SWCNTs having values over 3000 W/m·K. The strong dependence on diameter and chirality shows how phonons move in one dimension.

5. Interatomic Potentials for Simulating Carbon

Choosing the right interatomic potential is probably the most important methodological choice in carbon MD simulations. The wrong choice can change thermal conductivity predictions by up to four times and have a huge effect on how materials fail mechanically. This section critically assesses the principal potential families and nascent machine learning methodologies

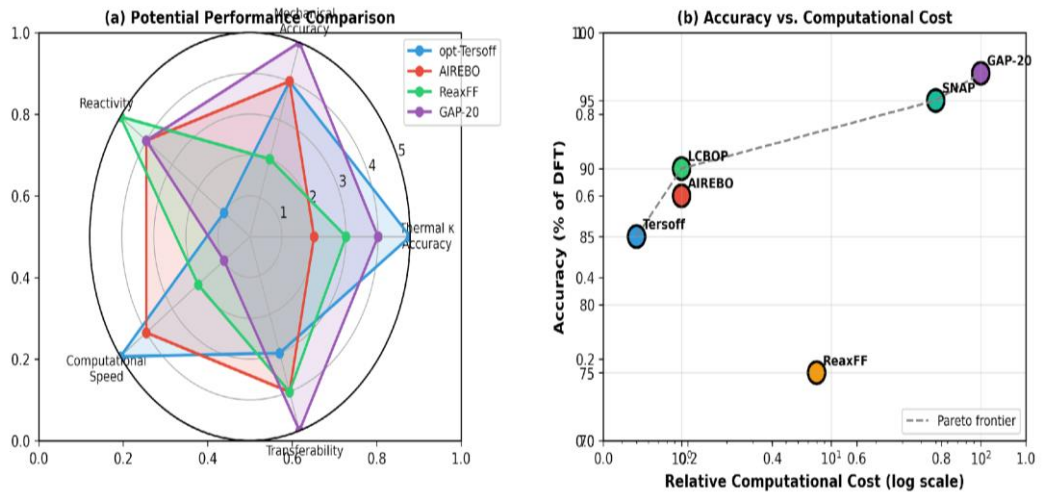

Figure 5: Interatomic potentials for carbon MD simulations: (a) Radar chart comparing potential performance across multiple criteria, (b) Accuracy versus computational cost trade-off showing the Pareto frontier

5.1 Empirical Bond-Order Potentials

The Tersoff potential and its derivatives are still very important for carbon simulations. They show the potential energy as a sum of pairwise interactions that is changed by a bond-order term that shows the local coordination environment. Lindsay and Broido's (2010) optimised Tersoff parameterisation give the best predictions for the thermal conductivity of graphene and CNTs. It accurately reproduces phonon dispersion relations and the inverse-square frequency dependence of phonon lifetimes. Standard Tersoff potentials, on the other hand, don't take into account long-range interactions and can't explain how bonds break and form during a fracture.

The Adaptive Intermolecular Reactive Empirical Bond Order (AIREBO) potential enhances REBO by incorporating torsional interactions and Lennard-Jones terms for non-bonded interactions, facilitating the simulation of multi-layer graphene and polymer composites. AIREBO does a better job of predicting how materials will break than other methods, with a Young's modulus of about 910 GPa. However, it greatly underestimates thermal conductivity because its acoustic phonon modes are too soft. The switching function used to break bonds causes unrealistic force spikes at intermediate bond distances. This led to the development of screened Tersoff variants (Tersoff-S) that make failure happen more smoothly.

5.2 Machine Learning Potentials

Machine learning interatomic potentials signify a revolutionary progression, attaining near-quantum mechanical precision at computational expenses suitable for extensive molecular dynamics simulations. Csányi and his team created the Gaussian Approximation Potential (GAP) framework, which uses smooth overlap of atomic positions (SOAP) descriptors with Gaussian process regression to get energy root-mean-square errors of about 10 meV/atom. The carbon GAP-20 potential, which was trained on 16,906 density functional theory configurations that included bulk phases, defects, and amorphous structures, gets more than 95% of the DFT cohesive energy accuracy and lets you run nanosecond simulations of million-atom systems.

The Spectral Neighbour Analysis Potential (SNAP) is a different way to use machine learning that works well in very harsh conditions. The carbon SNAP potential allows for simulations at 5 TPa pressure and 20,000 K temperature, with phase diagram accuracy within 3% of quantum molecular dynamics. This enables billion-atom simulations pertinent to

shock physics and planetary interior conditions. Neural network potentials like DeepMD and MACE provide more Pareto-optimal accuracy-speed trade-offs for certain uses. Active learning workflows (DP-GEN) automate the process of making training sets.

Table 3: Interatomic Potential Performance Comparison

Potential	κ Accuracy	E Accuracy	Reactivity	Relative Cost	Best Use
opt-Tersoff	Excellent	Good	No	0.5×	Thermal
AIREBO	Underest.	Good	Yes	1×	Fracture
ReaxFF	Variable	Moderate	Yes (QEq)	5-10×	Chemistry
GAP-20	Good	Excellent	Yes	100×	High accuracy
SNAP	Excellent	Good	Yes	50×	Extreme P,T

6. Energy Storage Applications

Molecular dynamics simulations illuminate atomic-scale mechanisms underlying macroscopic energy storage performance across multiple device architectures including lithium-ion batteries, supercapacitors, hydrogen storage systems, and thermal management materials.

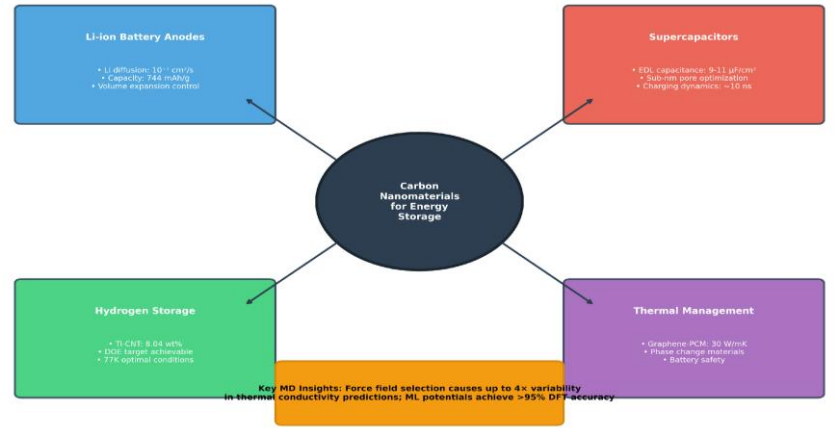

Figure 6: MD simulations for carbon-based energy storage systems showing four primary application domains: lithium-ion battery anodes, supercapacitors, hydrogen storage, and thermal management materials.

6.1 Lithium-Ion Battery Anodes

Graphite is still the most common anode material in commercial lithium-ion batteries. Lithium intercalation between graphene layers gives the battery a reversible capacity of 372 mAh/g, which is equal to the LiC_6 stoichiometry. MD simulations show that lithium diffusion coefficients can be anywhere from 10^{-6} to 10^{-16} cm²/s, depending on the method and the path of diffusion. In-plane diffusion parallel to graphene sheets attains rates of 10^{-7} to 10^{-6} cm²/s, whereas cross-plane diffusion through grain boundaries decreases to about 10^{-11} cm²/s, elucidating rate limitations in polycrystalline materials.

Silicon-graphene composites solve the problem of graphite's limited theoretical capacity by adding silicon, which has an amazing capacity of 3,579 mAh/g. MD simulations show that

graphene coatings cut silicon's huge volume expansion from 300–400% to about 67%, which slows down the mechanical degradation that causes capacity fade. Machine learning-driven MD finds that the amorphous silicon/graphite-I interface has the fastest lithiation rate, which helps optimise composite design. The Young's modulus of silicon diminishes from 100 GPa to 41 GPa during the transition to the $Li_{15}Si_4$ phase, elucidating the mechanisms of mechanical degradation.

6.2 Storing Hydrogen

The storage of hydrogen in carbon nanostructures has been systematically assessed through molecular dynamics and Monte Carlo simulations, focussing on the U.S. The Department of Energy's goal for practical vehicular uses is 6.5 wt% [128,129]. Physisorption in pristine CNTs meets this goal in wide-diameter open SWCNTs at 160 bar and 298 K. In cryogenic conditions (77 K), it can store up to 33 wt% for widely spaced narrow tubes. Metal decoration greatly improves storage: titanium-doped (12,12) CNTs reach 8.04 wt% at 77 K with 5% Ti doping—about four times more than undoped tubes—and keep more than 90% of their capacity after 100 cycles of adsorption and desorption.

6.3 Managing Heat

Thermal management simulations show that graphene could make batteries safer by helping them get rid of heat more quickly. Graphene-paraffin composites with 1 wt% graphene loading exhibit a 60-fold enhancement in thermal conductivity relative to unmodified paraffin phase change materials. Hyperbolic graphene-paraffin structures at 12.5 wt% reach a record 30.75 W/m·K while keeping 90% of their latent heat capacity. This makes it possible to stop thermal runaway at discharge rates of 3.75C. These materials keep the battery temperature stable at about 42°C phase transition points for more than 10,000 cycles.

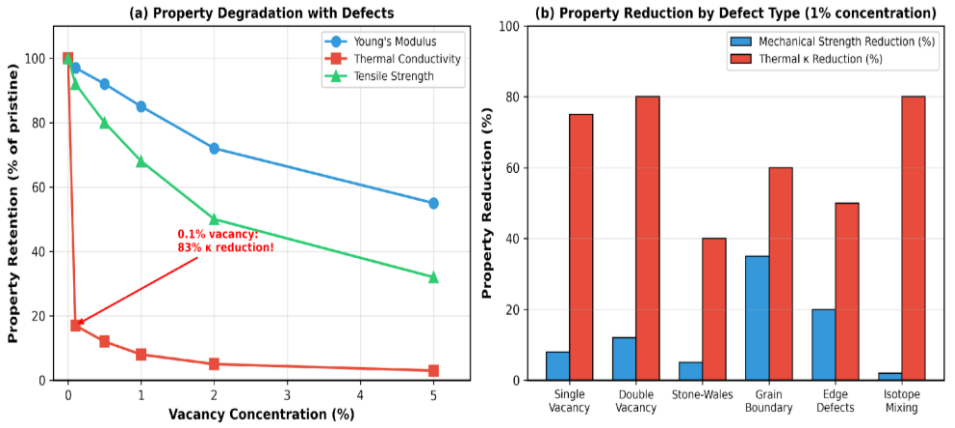

Figure 7: Impact of defects on carbon nanomaterial properties: (a) Property degradation with increasing vacancy concentration showing dramatic thermal conductivity reduction, (b) Comparison of property reduction by different defect types at 1% concentration.

Table 4: MD-Predicted Energy Storage Performance Parameters

Application	Material	Performance
Li-ion anode	Graphite	D_Li: 10^{-7}-10^{-6} cm²/s
Li-ion anode	Si-graphene	67% volume expansion
H_2 storage	Ti-CNT (5%)	8.04 wt% at 77 K
Supercapacitor	Carbide-derived C	~9 μF/cm²
Thermal mgmt.	Graphene-PCM	30.75 W/m·K

7. Future Research Directions

To make MD simulations more useful for designing materials for energy storage, there are a few important research gaps that need to be filled. First, the multiscale connection between atomistic MD (nanometre, nanosecond scales) and continuum models (device scale) is still not fully developed. The smoothed MD and Arlequin methods show promise, but there aren't any standard implementations of them yet. Second, most simulations use simplified defect structures, but real CVD-grown samples have complicated defect distributions that need stochastic defect modelling methods.

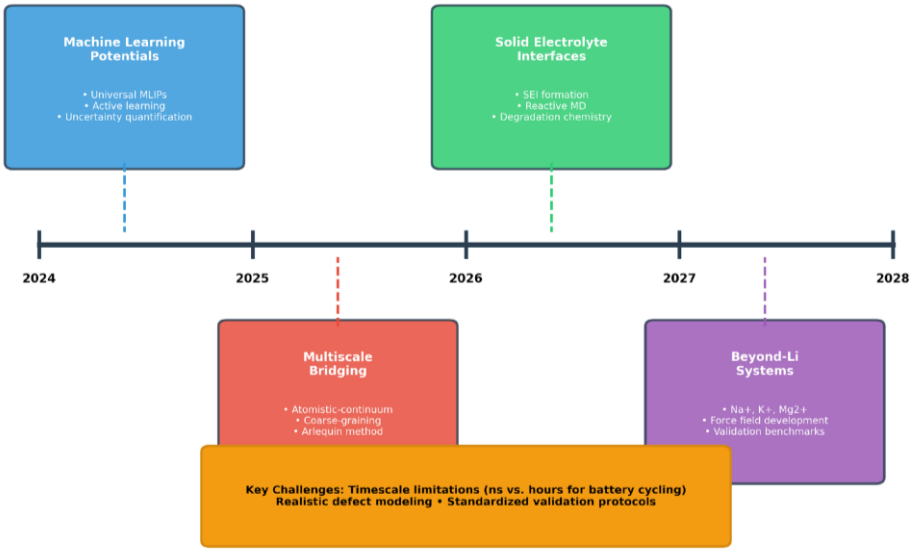

Figure 8: Future research directions in MD simulations for carbon energy materials showing the roadmap from 2024-2028 including machine learning potentials, multiscale bridging, solid electrolyte interfaces, and beyond-lithium systems.

Third, MD timescales (nanoseconds) cannot accurately represent the realistic dynamics of battery charge and discharge (seconds to hours), necessitating accelerated sampling techniques such as parallel replica dynamics, metadynamics, and kinetic Monte Carlo coupling. Fourth, the force fields for solid-electrolyte interfaces that are important for solid-state batteries are not as well-defined as those for liquid electrolyte systems. This means that they need to be systematically developed and tested. Fifth, beyond-lithium systems that use carbon anodes and sodium, potassium, magnesium, and aluminium ions need systematic force field development that has been tested against experimental benchmarks.

Machine learning potentials fix problems with accuracy, but they also create new problems, such as how to generalise training sets, how to measure uncertainty, and how to break bonds accurately. Active learning workflows automate the creation of training sets, but they need to be carefully checked for certain target properties. Combining machine learning with reactive potentials for forming and breaking down solid-electrolyte interfaces is a very promising area of research that could lead to predictive simulations of how batteries age.

8. Conclusions

This thorough review shows that molecular dynamics simulation is a well-established and important way to use computers to predict the properties of carbon nanomaterials that are important for energy storage applications. The synthesis of literature from 2020-2024 uncovers several significant findings. Pristine graphene has amazing mechanical properties, with a Young's modulus of 1.0 TPa and thermal conductivity of 5000 W/m·K for suspended samples. However, defect concentrations as low as 0.1% can lower thermal conductivity by 83%, which shows how important defect engineering is. Second, choosing interatomic potentials can change predictions of thermal conductivity by up to four times. Optimised Tersoff potentials are better for phonon transport, while AIREBO is still the best choice for fracture mechanics simulations.

Third, machine learning potentials like GAP-20 and SNAP now reach more than 95% of the accuracy of density functional theory at a much lower cost, making large-scale simulations possible that quantum mechanical methods couldn't handle before. Fourth, MD simulations show that titanium-coated carbon nanotubes can store 8.04 wt% of hydrogen at 77 K, which is more than the DOE's goals. Also, lithium diffusion coefficients in graphite electrodes can vary by six orders of magnitude depending on the diffusion pathway. Fifth, graphene-based phase change composites have thermal conductivities of 30.75 W/m·K while keeping their latent heat capacity, which makes them good for battery safety.

Important areas of research that need more work include creating standardised validation protocols, multiscale bridging methods that connect atomistic and continuum descriptions, reactive force fields for solid-electrolyte interfaces, and systematic force field development for battery chemistries that go beyond lithium. The ongoing fusion of machine learning techniques with conventional molecular dynamics methods is expected to expedite the computational discovery of materials for next-generation energy storage systems. To fully realise the potential of MD simulation for rational material design, future progress will require coordinated efforts that include developing algorithms, building high-performance computing infrastructure, and systematically validating experiments.

References

[1]. Yang, Z., Zhang, J., Kintner-Meyer, M. C. W., et al. (2011). Electrochemical energy storage for green grid. *Chemical Reviews, 111*(5), 3577–3613.
[2]. Dunn, B., Kamath, H., & Tarascon, J. M. (2011). Electrical energy storage for the grid: A battery of choices. *Science, 334*(6058), 928–935.
[3]. Goodenough, J. B., & Park, K. S. (2013). The Li-ion rechargeable battery: A perspective. *Journal of the American Chemical Society, 135*(4), 1167–1176.
[4]. Novoselov, K. S., Geim, A. K., Morozov, S. V., et al. (2004). Electric field effect in atomically thin carbon films. *Science, 306*(5696), 666–669.
[5]. Geim, A. K., & Novoselov, K. S. (2007). The rise of graphene. *Nature Materials, 6*(3), 183–191.
[6]. Iijima, S. (1991). Helical microtubules of graphitic carbon. *Nature, 354*(6348), 56–58.
[7]. Balandin, A. A., Ghosh, S., Bao, W., et al. (2008). Superior thermal conductivity of single-layer graphene. *Nano Letters, 8*(3), 902–907.
[8]. Bolotin, K. I., Sikes, K. J., Jiang, Z., et al. (2008). Ultrahigh electron mobility in

suspended graphene. *Solid State Communications, 146*(9–10), 351–355.

[9]. Lee, C., Wei, X., Kysar, J. W., & Hone, J. (2008). Measurement of the elastic properties and intrinsic strength of monolayer graphene. *Science, 321*(5887), 385–388.

[10]. Yu, M. F., Files, B. S., Arepalli, S., & Ruoff, R. S. (2000). Tensile loading of ropes of single wall carbon nanotubes. *Physical Review Letters, 84*(24), 5552–5555.

[11]. Dresselhaus, M. S., Dresselhaus, G., Saito, R., & Jorio, A. (2005). Raman spectroscopy of carbon nanotubes. *Physics Reports, 409*(2), 47–99.

[12]. De Volder, M. F., Tawfick, S. H., Baughman, R. H., & Hart, A. J. (2013). Carbon nanotubes: Present and future commercial applications. *Science, 339*(6119), 535–539.

[13]. Alder, B. J., & Wainwright, T. E. (1959). Studies in molecular dynamics. I. General method. *Journal of Chemical Physics, 31*(2), 459–466.

[14]. Rahman, A. (1964). Correlations in the motion of atoms in liquid argon. *Physical Review, 136*(2A), A405–A411.

[15]. Car, R., & Parrinello, M. (1985). Unified approach for molecular dynamics and density-functional theory. *Physical Review Letters, 55*(22), 2471–2474.

[16]. Allen, M. P., & Tildesley, D. J. (2017). *Computer simulation of liquids* (2nd ed.). Oxford University Press.

[17]. Frenkel, D., & Smit, B. (2023). *Understanding molecular simulation: From algorithms to applications* (3rd ed.). Academic Press.

[18]. Thompson, A. P., Aktulga, H. M., Berger, R., et al. (2022). LAMMPS - a flexible simulation tool for particle-based materials modeling. *Computer Physics Communications, 271*, 108171.

[19]. Plimpton, S. (1995). Fast parallel algorithms for short-range molecular dynamics. *Journal of Computational Physics, 117*(1), 1–19.

[20]. Rapaport, D. C. (2004). *The art of molecular dynamics simulation* (2nd ed.). Cambridge University Press.

[21]. Stuart, S. J., Tutein, A. B., & Harrison, J. A. (2000). A reactive potential for hydrocarbons with intermolecular interactions. *Journal of Chemical Physics, 112*(14), 6472–6486.

[22]. Brenner, D. W., Shenderova, O. A., Harrison, J. A., et al. (2002). A second-generation reactive empirical bond order (REBO) potential. *Journal of Physics: Condensed Matter, 14*(4), 783–802.

[23]. van Duin, A. C. T., Dasgupta, S., Lorant, F., & Goddard, W. A. (2001). ReaxFF: A reactive force field for hydrocarbons. *Journal of Physical Chemistry A, 105*(41), 9396–9409.

[24]. Tersoff, J. (1989). Modeling solid-state chemistry: Interatomic potentials for multicomponent systems. *Physical Review B, 39*(8), 5566–5568.

[25]. Katoch, S., Chauhan, S. S., & Kumar, V. (2021). A review on genetic algorithm: Past, present, and future. *Multimedia Tools and Applications, 80*(5), 8091–8126.

[26]. Mortazavi, B., Podryabinkin, E. V., Novikov, I. S., et al. (2021). Accelerating first-principles estimation of thermal conductivity by machine learning. *Materials Today, 47*, 20–28.

[27]. Zhu, T., & Ertekin, E. (2016). Phonons, localization, and thermal conductivity of diamond nanothreads and amorphous graphene. *Nano Letters, 16*(8), 4763–4772.

[28]. Verlet, L. (1967). Computer experiments on classical fluids. I. Thermodynamical properties of Lennard-Jones molecules. *Physical Review, 159*(1), 98–103.

[29]. Swope, W. C., Andersen, H. C., Berens, P. H., & Wilson, K. R. (1982). A computer simulation method for the calculation of equilibrium constants. *Journal of Chemical Physics, 76*(1), 637–649.

[30]. Tuckerman, M. E., Berne, B. J., & Martyna, G. J. (1992). Reversible multiple time scale molecular dynamics. *Journal of Chemical Physics, 97*(3), 1990–2001.

[31]. Hess, B., Bekker, H., Berendsen, H. J. C., & Fraaije, J. G. E. M. (1997). LINCS: A linear constraint solver for molecular simulations. *Journal of Computational Chemistry, 18*(12), 1463–1472.

[32]. Ryckaert, J. P., Ciccotti, G., & Berendsen, H. J. C. (1977). Numerical integration of cartesian equations of motion. *Journal of Computational Physics, 23*(3), 327–341.

[33]. Brown, W. M., Wang, P., Plimpton, S. J., & Tharrington, A. N. (2011). Implementing molecular dynamics on hybrid high

performance computers. *Computer Physics Communications, 182*(4), 898–911.

[34]. Aktulga, H. M., Fogarty, J. C., Pandit, S. A., & Grama, A. Y. (2012). Parallel reactive molecular dynamics: Numerical methods and algorithmic techniques. *Parallel Computing, 38*(4–5), 245–259.

[35]. Nguyen, T. D., Phillips, C. L., Anderson, J. A., & Glotzer, S. C. (2011). Rigid body constraints realized in massively-parallel molecular dynamics. *Computer Physics Communications, 182*(11), 2307–2313.

[36]. Abraham, M. J., Murtola, T., Schulz, R., et al. (2015). GROMACS: High performance molecular simulations through multi-level parallelism. *SoftwareX, 1–2*, 19–25.

[37]. Case, D. A., Cheatham, T. E., Darden, T., et al. (2005). The Amber biomolecular simulation programs. *Journal of Computational Chemistry, 26*(16), 1668–1688.

[38]. Nosé, S. (1984). A unified formulation of the constant temperature molecular dynamics methods. *Journal of Chemical Physics, 81*(1), 511–519.

[39]. Hoover, W. G. (1985). Canonical dynamics: Equilibrium phase-space distributions. *Physical Review A, 31*(3), 1695–1697.

[40]. Martyna, G. J., Klein, M. L., & Tuckerman, M. (1992). Nosé-Hoover chains: The canonical ensemble via continuous dynamics. *Journal of Chemical Physics, 97*(4), 2635–2643.

[41]. Parrinello, M., & Rahman, A. (1981). Polymorphic transitions in single crystals: A new molecular dynamics method. *Journal of Applied Physics, 52*(12), 7182–7190.

[42]. Berendsen, H. J. C., Postma, J. P. M., van Gunsteren, W. F., et al. (1984). Molecular dynamics with coupling to an external bath. *Journal of Chemical Physics, 81*(8), 3684–3690.

[43]. Liu, Y., & Chen, X. (2014). Mechanical properties of nanoporous graphene membrane. *Journal of Applied Physics, 115*(3), 034303.

[44]. Zhang, Y. Y., Wang, C. M., Cheng, Y., & Xiang, Y. (2011). Mechanical properties of bilayer graphene sheets coupled by sp^3 bonding. *Carbon, 49*(13), 4511–4517.

[45]. Rajasekaran, G., Narayanan, P., & Parashar, A. (2016). Effect of point and line defects on mechanical and thermal properties of graphene. *Critical Reviews in Solid State and Materials Sciences, 41*(1), 47–71.

[46]. Mortazavi, B., & Rabczuk, T. (2015). Multiscale modeling of heat conduction in graphene laminates. *Carbon, 85*, 1–7.

[47]. Wei, Y., Wang, B., Wu, J., et al. (2013). Bending rigidity and Gaussian bending stiffness of single-layered graphene. *Nano Letters, 13*(1), 26–30.

[48]. Zhao, H., & Aluru, N. R. (2010). Temperature and strain-rate dependent fracture strength of graphene. *Journal of Applied Physics, 108*(6), 064321.

[49]. Min, K., & Aluru, N. R. (2011). Mechanical properties of graphene under shear deformation. *Applied Physics Letters, 98*(1), 013113.

[50]. Dewapriya, M. A. N., Rajapakse, R. K. N. D., & Phani, A. S. (2014). Atomistic and continuum modelling of temperature-dependent fracture of graphene. *International Journal of Fracture, 187*(2), 199–212.

[51]. Zhang, B., Mei, L., & Xiao, H. (2012). Nanofracture in graphene under complex mechanical stresses. *Applied Physics Letters, 101*(12), 121915.

[52]. Khare, R., Mielke, S. L., Paci, J. T., et al. (2007). Coupled quantum mechanical/molecular mechanical modeling of the fracture of defective carbon nanotubes. *Physical Review B, 75*(7), 075412.

[53]. Jaddi, S., Coulombier, M., Raskin, J. P., & Pardoen, T. (2024). Definitive engineering strength and fracture toughness of graphene. *Nature Communications, 15*, 1–9.

[54]. Yin, H., Qi, H. J., Fan, F., et al. (2015). Griffith criterion for brittle fracture in graphene. *Nano Letters, 15*(3), 1918–1924.

[55]. Yakobson, B. I., Brabec, C. J., & Bernholc, J. (1996). Nanomechanics of carbon tubes: Instabilities beyond linear response. *Physical Review Letters, 76*(14), 2511–2514.

[56]. Ozaki, T., Iwasa, Y., & Mitani, T. (2000). Stiffness of single-walled carbon nanotubes under large strain. *Physical Review Letters, 84*(8), 1712–1715.

[57]. Bai, X., Liao, S., Chen, S., et al. (2017). Tensile properties of millimeter-long

multi-walled carbon nanotubes. *Scientific Reports, 7*, 10279.

[58]. Peng, B., Locascio, M., Zapol, P., et al. (2008). Measurements of near-ultimate strength for multiwalled carbon nanotubes. *Nature Nanotechnology, 3*(10), 626–631.

[59]. Song, Z., Artyukhov, V. I., Yakobson, B. I., & Xu, Z. (2013). Pseudo Hall-Petch strength reduction in polycrystalline graphene. *Nano Letters, 13*(4), 1829–1833.

[60]. Cao, A., & Qu, J. (2013). Atomistic simulation study of brittle failure in nanocrystalline graphene under uniaxial tension. *Applied Physics Letters, 102*(7), 071902.

[61]. Fthenakis, Z. G., Zhu, Z., & Tománek, D. (2014). Effect of structural defects on the thermal conductivity of graphene. *Physical Review B, 89*(12), 125421.

[62]. Hao, F., Fang, D., & Xu, Z. (2011). Mechanical and thermal transport properties of graphene with defects. *Applied Physics Letters, 99*(4), 041901.

[63]. Zheng, Q., Geng, Y., Wang, S., et al. (2012). Molecular dynamics study of the effect of chemical functionalization on mechanical properties of graphene. *Journal of Applied Physics, 111*(12), 124314.

[64]. Deng, S., & Berry, V. (2016). Wrinkled, rippled and crumpled graphene: An overview of formation mechanism. *Materials Today, 19*(4), 197–212.

[65]. Voter, A. F. (1997). Hyperdynamics: Accelerated molecular dynamics of infrequent events. *Physical Review Letters, 78*(20), 3908–3911.

[66]. Laio, A., & Parrinello, M. (2002). Escaping free-energy minima. *Proceedings of the National Academy of Sciences USA, 99*(20), 12562–12566.

[67]. Mortazavi, B., & Ahzi, S. (2013). Thermal conductivity and tensile response of defective graphene: A molecular dynamics study. *Carbon, 63*, 460–470.

[68]. Jing, N., Xue, Q., Ling, C., et al. (2012). Effect of defects on Young's modulus of graphene sheets: A molecular dynamics simulation. *RSC Advances, 2*(24), 9124–9129.

[69]. Kubo, R. (1957). Statistical-mechanical theory of irreversible processes. *Journal of the Physical Society of Japan, 12*(6), 570–586.

[70]. Green, M. S. (1954). Markoff random processes and the statistical mechanics of time-dependent phenomena. *Journal of Chemical Physics, 22*(3), 398–413.

[71]. Schelling, P. K., Phillpot, S. R., & Keblinski, P. (2002). Comparison of atomic-level simulation methods for computing thermal conductivity. *Physical Review B, 65*(14), 144306.

[72]. Sellan, D. P., Landry, E. S., Turney, J. E., et al. (2010). Size effects in molecular dynamics thermal conductivity predictions. *Physical Review B, 81*(21), 214305.

[73]. Fan, Z., Pereira, L. F. C., Wang, H. Q., et al. (2015). Force and heat current formulas for many-body potentials in molecular dynamics simulations. *Physical Review B, 92*(9), 094301.

[74]. Thomas, J. A., Turney, J. E., Iber, R. M., et al. (2010). Predicting phonon dispersion relations and lifetimes from the spectral energy density. *Physical Review B, 81*(8), 081411.

[75]. Müller-Plathe, F. (1997). A simple nonequilibrium molecular dynamics method for calculating the thermal conductivity. *Journal of Chemical Physics, 106*(14), 6082–6085.

[76]. Jund, P., & Jullien, R. (1999). Molecular-dynamics calculation of the thermal conductivity of vitreous silica. *Physical Review B, 59*(21), 13707–13711.

[77]. Evans, D. J. (1982). Homogeneous NEMD algorithm for thermal conductivity. *Physics Letters A, 91*(9), 457–460.

[78]. Swartz, E. T., & Pohl, R. O. (1989). Thermal boundary resistance. *Reviews of Modern Physics, 61*(3), 605–668.

[79]. Kapitza, P. L. (1941). The study of heat transfer in helium II. *Journal of Physics USSR, 4*, 181–210.

[80]. Ghosh, S., Calizo, I., Teweldebrhan, D., et al. (2008). Extremely high thermal conductivity of graphene. *Applied Physics Letters, 92*(15), 151911.